0026-895X/99/010179-07$3.00/0

MOLECULAR PHARMACOLOGY, **55:**179–185 (1999).

Site-Directed Mutagenesis of Predicted Active Site Residues in Glutamate Carboxypeptidase II

HENRY S. SPENO, RUTH LUTHI-CARTER, WENDY L. MACIAS, STACEY L. VALENTINE, AMIT R. T. JOSHI, and JOSEPH T. COYLE

Laboratory of Molecular and Developmental Neuroscience, Massachusetts General Hospital-East, Charlestown, Massachusetts

Received August 3, 1998; accepted October 19, 1998

This paper is available online at http://www.molpharm.org

ABSTRACT

Glutamate carboxypeptidase II (GCP II) catalyzes the extracellular hydrolysis of the neuromodulator *N*-acetyl-aspartylglutamate to *N*-acetyl-aspartate and glutamate. GCP II also hydrolyzes γ-glutamyl bonds in folylpolyglutamate. The predicted amino acid sequence of GCP II displays similarities to aminopeptidases from *Streptomyces griseus* and *Vibrio proteolyticus*, whose crystal structures have been determined. These aminopeptidases are cocatalytic zinc metallopeptidases belonging to the peptidase family M28. Specific zinc and substrate ligands have been proposed in GCP II based on the amino acid sequence alignment to these M28 family members. In the present study, site-directed mutagenesis has been used to test the assignment of these putative ligands in human GCP II. Substitutions to the five putative zinc ligands resulted in severely reduced enzyme activity, although mutant protein was expressed as demonstrated by immunoblot analysis. In addition, substitutions of amino acids near the putative zinc ligands have identified other specific residues important for enzyme structure and/or function. Substitutions to putative substrate ligands were less perturbing, and increases in K_m were observed for substitutions that introduced a large charge perturbation (e.g., Lys to Glu). The results from substitutions at the proposed zinc and substrate ligands are consistent with the assignment of these residues and suggest that GCP II has a three-dimensional structure similar to other members of the peptidase family M28.

Glutamate carboxypeptidase II (GCP II) hydrolyzes the abundant neuropeptide *N*-acetyl-aspartylglutamate (NAAG) to *N*-acetyl-aspartate and glutamate in the extracellular space (Robinson et al., 1987; Stauch et al., 1989; Serval et al., 1990; Slusher et al., 1990). NAAG inhibits glutamate's activation of the *N*-methyl-D-aspartate ionotropic receptor (Sekiguchi et al., 1989; Puttfarcken et al., 1993; Burlina et al., 1994; Grunze et al., 1996) and is an agonist at the metabotropic glutamate receptor mGluR3 (Wroblewska et al., 1997). GCP II terminates the action of NAAG and generates extrasynaptic glutamate in the brain. Inhibition of GCP II by 2-(phosphonomethyl)pentanedioic acid (PMPA), has been shown to be effective in preventing neuronal cell death in models of ischemia (Harukuni et al., 1997). GCP II also hydrolyzes γ-glutamyl linkages in pteroylpolyglutamate (Pinto et al., 1996). Conversion of pteroylpolyglutamate to pteroylmono-glutamate is necessary for intestinal absorption of folic acid.

GCP II is also expressed in selected sites outside the brain including nonmyelinating Schwann cells and the neuromuscular junction, small intestine, kidney, and prostate (Slusher et al., 1992; Berger et al., 1995a,b; Troyer et al., 1995a). At some of these peripheral sites, GCP II may act on substrates other than NAAG. The name glutamate carboxypeptidase II (EC 3.4.17.21) has been recently assigned; the enzyme has previously been called *N*-acetyl-α-linked acidic dipeptidase or NAALADase and prostate-specific membrane antigen or PSM. Molecular characterizations of rat, pig, and human forms of GCP II have been described (Israeli et al., 1993; Carter et al., 1996; Bzdega et al., 1997; Halsted et al., 1998; Luthi-Carter et al., 1998).

GCP II is a class II membrane glycoprotein with an apparent molecular mass of 94 to 100 kDa. Class II membrane proteins have a short cytoplasmic amino terminus, a single membrane-spanning domain, and a large extracellular domain (Fig. 1). A model for human GCP II has recently been proposed by Rawlings and Barrett (1997) based on a region of similarity to the peptidase family M28 comprised of cocatalytic metallopeptidases. The catalytic domain of GCP II (Fig. 1) has been identified by sequence similarities to low molecular weight aminopeptidases from *Streptomyces griseus* and *Vibrio proteolyticus* (also known as *Aeromonas proteolytica*). The X-ray crystal structures have been determined for the

This work was supported by National Association for Research on Schizophrenia and Affective Disorders Hilton Senior Investigator Award (to J.T.C.), National Research Service Award fellowships from the National Institute of Mental Health 5-T32-MH14275–21 (to B.K. Madras), and 1 F32 MH11895–01 (to H.S.S.).

ABBREVIATIONS: GCP II, glutamate carboxypeptidase II; NAAG, *N*-acetyl-aspartylglutamate; NEP, neutral endopeptidase; PMPA, 2-(phosphonomethyl)pentanedioic acid.

Streptomyces and *Vibrio* aminopeptidases at 1.75-Å and 1.8-Å resolution, respectively (Chevrier et al., 1994; Greenblatt et al., 1997). These peptidases have a binuclear Zn^{++} center at the active site in which the two zinc ions share a bridging carboxylate ligand. In addition, the structure of carboxypeptidase G_2 has been determined at 2.5-Å resolution and has a central topology quite similar to the *Vibrio* aminopeptidase, even though no significant amino acid sequence identity exists (Rowsell et al., 1997). Carboxypeptidase G_2 hydrolyzes the α-linked glutamate from folic acid. The binuclear zinc-binding sites found in carboxypeptidase G_2 and the *Vibrio* aminopeptidase are highly similar in structure and ligand environment (Table 1).

To test amino acid assignments, putative ligands for Zn^{++} in GCP II have been targeted for amino acid substitution based on the alignment of the amino acid sequence to the *Streptomyces* and *Vibrio* aminopeptidases. The five putative Zn^{++} ligands and their positions in GCP II are: His-377, Asp-387, Glu-425, Asp-453, and His-553, where Asp-387 is predicted to be the bridging ligand (Table 1). In contrast to both structural and catalytic mono-zinc sites, carboxylate oxygen coordination predominates in binuclear zinc sites (Vallee and Auld, 1993).

The crystal structure of the *Vibrio* aminopeptidase shows 10 residues lining a hydrophobic specificity pocket implicated in substrate binding (Chevrier et al., 1994). In the amino acid sequence alignment, Rawlings and Barrett (1997) noted that four of the residues that line the specificity pocket of the *Vibrio* enzyme are substituted by positively charged residues (i.e., Arg-463, Lys-499, Arg-536, and Lys-545), which may account in part for substrate specificity in GCP II (Table 2). These and some of the other 10 predicted substrate ligands, a subset of which are next to putative zinc ligands, have been targeted for amino acid substitution (Tables 1 and 2).

Materials and Methods

Site-Directed Mutagenesis. The cDNA for human GCP II has been subcloned into the mammalian expression vector, pcDNA3 (Invitrogen Corporation, Carlsbad, CA). Single-stranded template was used in an in vitro mutagenesis reaction according to Kunkel et al. (1991). When possible, restriction sites were designed into or out of the mutation site to facilitate screening. Mutations were confirmed by DNA sequencing.

Radioenzymatic Assay of Enzyme Activity. To test for alterations in function of the encoded proteins, plasmids containing the confirmed mutations were transiently transfected into the prostate cancer cell line PC3 (American Type Culture Collection, Rockville, MD), which does not express endogenous GCP II activity or protein (Carter et al., 1996). Transfections were carried out following a calcium phosphate method in 50 mM HEPES, pH 7.05 (Graham and van der Eb, 1973). After incubation for 48 h, cells were harvested at 4°C and sonicated in the presence of 50 mM Tris, pH 7.4, 0.5% Triton X-100 in high-pressure liquid chromatography grade H_2O. Cell lysates were then incubated in the presence of the radiolabeled substrate *N*-acetyl-L-aspartyl-L-[3,4-^{3}H]glutamate (NEN Life Science Products, Boston, MA). Products were separated from intact substrate using disposable anion exchange columns and L-[3,4-^{3}H]glutamate measured by scintillation spectrometry as described in a study by Robinson et al. (1987). Enzymatic activity of GCP II in 2 μg of total protein from the cell lysate was assayed in a final volume of 250 μl using 30 nM *N*-acetyl-L-aspartyl-L-[3,4-^{3}H]glutamate in 50 mM Tris, pH 7.4, at 37°C, 0.1% Triton X-100, 150 μM potassium phosphate, and 1 mM $CoCl_2$ (Robinson et al., 1987). Total protein was assayed using the bicinchoninic acid assay (Pierce, Rockford, IL). To test for metal ion dependence of mutant enzyme activity, activity was recovered by the addition of Co^{++} or Zn^{++} in the presence of EDTA (Robinson et al., 1987). Because all transfects were expressed in the same cell system, it is assumed that differences in kinetic characteristics reflect primarily the transfected species.

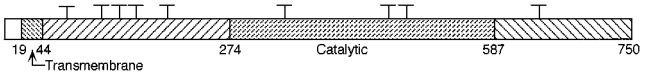

Fig. 1. Primary structure of GCP II. The individual predicted domains are drawn to scale demonstrating a short cytoplasmic domain, a single membrane spanning domain based on hydropathy profiles, and a large extracellular domain with nine potential *N*-glycosylation sites each indicated by a "T". Amino acid positions are indicated below at the end of each region. The catalytic domain is predicted by similarities to aminopeptidases from *S. griseus* and *V. proteolyticus* (Rawlings and Barrett, 1997).

Kinetic Analysis. For those mutants that showed activity, Michaelis-Menten (saturation) kinetics were performed. The K_m and V_{max} parameters were determined by a nonlinear least-squares fit of the initial velocity versus substrate concentration plot using Prism software (GraphPad, San Diego, CA) where the error in these parameters is represented by the 95% confidence interval. At each substrate concentration, three time points were taken either at 15, 30, and 45 min for wild type or up to 120, 180, and 240 min for mutants within the linear range of the assay. Background counts from the coelution of intact substrate were subtracted from each point by including a sample without enzyme. The concentration of the labeled substrate [^{3}H]NAAG was kept constant at 30 nM, whereas the concentration of unlabeled substrate was varied from 100 to 3000 nM. The initial velocity, v (in femtomoles per minute), at a given substrate concentration was determined from the slope of the linear plot of product versus time where the error in the initial velocity is represented by the S.E.M. of the 95% confidence interval from the linear regression of the slope. To compare changes in V_{max} between mutant and wild-type enzymes, the V_{max} parameter has been normalized by the ratio of wild-type to mutant protein from the relative intensity of the signal measured from an immunoblot (see below).

Inhibitor Analysis. Activity of selected mutants was measured in the presence of varying concentrations of inhibitors in a volume of 125 μl using 2 μg of total protein, 1 mM $CoCl_2$, and 10 nM [^{3}H]NAAG. PMPA was a gift from Dr. Barbara Slusher (Guilford Pharmaceuticals, Baltimore, MD). Pteroylpenta-γ-glutamate was purchased from B. Schircks Laboratories (Jona, Switzerland). [^{3}H]NAAG is shipped in phosphate buffer, however phosphate inhibition of GCP II did not interfere with kinetic analysis at the concentration of [^{3}H]NAAG used. To exchange the buffer for inhibitor analysis and to purify *N*-acetyl-L-aspartyl-L-[3,4-^{3}H]glutamate (NEN Life Science Products), up to 250 μl of 24 μM [^{3}H]NAAG was applied to a 1-ml bed volume of anion exchange resin AG 1-X8 (Bio-Rad, Hercules, CA), washed with 3 ml of 1 M formic acid, and eluted in 3 ml of 7.5 M formic acid. The sample was lyophilized and resuspended in 3 ml of H_2O and lyophilized two more times. The pellet was resuspended in 200 mM Tris, pH 9.5, and if necessary, the pH adjusted to 7.0 with NaOH.

Immunoblot Analysis. To normalize for the amount of enzyme used between wild type and mutants in the kinetic assays, the relative amount of GCP II protein was quantitated by immunoblotting (Western blot analysis). Cellular lysates were separated by 7% SDS-polyacrylamide gel electrophoresis, transferred to nitrocellulose in 10 mM 3-cyclohexylamino-1-propane sulfonic acid, pH 11, 1% methanol, and probed with the monoclonal antibody 7E11-C5 at 3 μg/ml (a generous gift from Drs. Gerald Murphy and Alton Boynton) (Israeli et al., 1994). The 7E11-C5 antibody recognizes the N terminus of GCP II (Troyer et al., 1995b). Because no mutations were near this epitope, amino acid substitutions were not expected to interfere with binding of the antibody. Horseradish peroxide-conjugated sec-

ondary antibody (Jackson ImmunoResearch Laboratories, Inc., West Grove, PA) was used to visualize the complex in conjunction with the chemiluminescent substrate SuperSignal ULTRA (Pierce). Data were collected with a Fluor-S MultiImager (Bio-Rad) and analyzed by Multi-Analyst software (Bio-Rad). To test that the immunoblot was linear in the range of experimental samples, the intensities were measured as a function of time. The amount of GCP II protein is expressed per microgram of total protein loaded. For qualitative analysis, immunoblots were visualized using film autoradiography.

Deglycosylation of Native Protein. To characterize the two bands observed in the immunoblot of transiently expressed GCP II, samples were deglycosylated under denaturing conditions with peptide-*N*-glycosidase according to the manufacturer's recommended protocol (Oxford GlycoSciences, Inc., Bedford, MA) and probed with 7E11-C5 antibody in an immunoblot as described above.

Results

Substitutions to Putative Zinc Ligands. Based on amino acid sequence alignment to other cocatalytic zinc peptidases of the M28 family, the catalytic domain and potentially important functional groups have been identified in GCP II (Rawlings and Barrett, 1997). Site-directed mutagenesis has been used to test the assignment of specific amino acid residues implicated in zinc and substrate binding. Single substitutions to putative zinc ligands resulted in a profound loss of enzyme activity (Table 3). The severe loss of activity in these mutants is not due to the inability of transfectants to express GCP II protein, as determined by immunoblot analysis (examples shown in Fig. 2A). However, reduced expression was observed for some of these mutants (Table 3). The only mutant in which kinetic parameters were obtainable was D387N, a substitution at the putative bridging ligand that resulted in both an increased K_m value and a decreased V_{max} when compared with wild type (Fig. 3 and Table 4). The profile of activity versus metal ion concentration did not change for the D387N and E424Q (see below) mutants when compared with wild-type enzyme, suggesting that these substitutions did not disrupt metal binding (data not shown).

Substitutions to Residues Next to Putative Zinc Ligands. Substitutions to residues next to each of the five putative zinc ligands were also targeted. These included Asp-379, Pro-388, Glu-424, Ser-454, and Tyr-552. The following results are shown in Tables 3 and 4. 1) Conservative substitutions at Asp-379 resulted in no detectable enzyme activity (after a 16-h incubation) and in a reduced expression of protein, underscoring the importance of the structure in this region. In the *Streptomyces* and *Vibrio* aminopeptidases, the corresponding residue was hydrogen bonded to the nearby histidine zinc ligand. 2) Substitution of Pro-388 to Ala resulted in a large increase in K_m. It has been noted in binuclear zinc metallopeptidases that a *cis*-peptide bond occurs near one of the zinc ligands (Table 1). 3) The E424Q mutant resulted in a reduced V_{max} value along with an increase in K_m (Fig. 3 and Table 4). A glutamate implicated in catalysis is typically found next to one of the zinc ligands in both bi- and mononuclear zinc metallopeptidases (Rowsell et al., 1997). 4) The S454A mutant had a decrease in V_{max}. 5) The Y552F mutant had an increased K_m and decreased V_{max}. In the *Vibrio* and *Streptomyces* aminopeptidases the corresponding positions (Ser-454 and Tyr-552) are implicated as comprising part of the substrate binding pocket indicating proximity to the active site.

Substitutions to Putative Substrate Ligands. In contrast to substitutions to putative zinc ligands, single substitutions to putative substrate ligands were less disruptive to enzyme activity so that kinetic parameters could be obtained for most of the mutants. For the positively charged residues implicated in determining substrate specificity, including Lys-500, conservative substitutions that exchanged Lys for Arg did not markedly alter the kinetic parameters (Table 4). However, when the substitution introduced a large charge perturbation (e.g., Lys to Glu), the K_m for substrate of these mutants increased greatly. This was seen for the R463I, R536E, and K545E mutants (Table 4, an example of which is shown in Fig. 3A). Immunoblot analysis indicates that the expression of these mutants is like wild type except that the upper band is faint for the R463I mutant (data not shown). No activity was detected for the K500E mutant (after a 16-h incubation), and reduced expression was observed in an immunoblot (Fig. 2A). Little change in the kinetic parameters was seen for the K499E and S501A mutants, even though they are directly next to Lys-500, which has no activity when substituted to Glu. Very little activity was seen for the N519D mutant after a 16-h incubation, so kinetic parameters could not be obtained. Finally, the T538V mutant had a large increase in the K_m parameter (Table 4). Residues corresponding to Asn-519 and Thr-538 have been implicated in contributing to the substrate binding pocket of the aminopeptidases.

Enzyme Activity in the Presence of Inhibitors. To further analyze mutants that may affect substrate binding, [^{3}H]NAAG hydrolysis was measured in the presence of in-

TABLE 1

Putative zinc ligands and nearby residues targeted for substitution in GCP II

Amino acids targeted for substitution were based on comparison with the following proteins of known structure: aminopeptidases from S. griseus and V. proteolyticus, and carboxypeptidase G_2, CPG2 (Greenblatt et al., 1997; Chevrier et al., 1994; Rowsell et al., 1997). Interactions of residues with Zn^{2+}, Hg^{2+}, $H_2PO_4^-$, and hydroxamate that were observed in the crystal structures are indicated under "Comments". Based on the alignment, certain predictions can be made: Asp-379 is proposed to hydrogen bond to the putative zinc ligand His-377. Asp-387 is the putative bridging ligand. Pro-388 is proposed to be involved in a cis-peptide bond with Asp-387. Glu-424 is predicted to be involved in catalysis.

GCP II	*Streptomyces*	*Vibrio*	CPG2	Comments
His-377	His-85	His-97	His-112	Zn^{2+}/Hg^{2+}
Asp-379	Asp-87	Asp-99	Asp-114	H-bond
Asp-387	Asp-97	Asp-117	Asp-141	Zn^{2+}/Hg^{2+} bridging
Pro-388	Asn-98	Asp-118	Asp-142	cis bond
Glu-424	Glu-131	Glu-151	Glu-175	$H_2PO_4^-$/hydroxamate
Glu-425	Glu-132	Glu-152	Glu-176	Zn^{2+}
Asp-453	Asp-160	Asp-179	Glu-200	Zn^{2+}/Hg^{2+}
Ser-454	Met-161	Met-180	Pro-201	
Tyr-552	Tyr-246	Ile-255	Tyr-384	$H_2PO_4^-$
His-553	His-247	His-256	His-385	Zn^{2+}

hibitors or the unlabeled alternative substrate, pteroylpenta-γ-glutamate (Pinto et al., 1996). The IC_{50} was determined for pteroylpenta-γ-glutamate in the presence of [^{3}H]NAAG for some of the mutants (Table 5). An 8- and 9-fold increase was seen in the IC_{50} for the R536E and K545E mutants, respectively (Table 5), consistent with their increased K_m for NAAG (Table 4). The Y552F mutant showed dramatic changes in the IC_{50} for PMPA, phosphate, glutamate, and pteroylpenta-γ-glutamate (Table 6), suggesting a role for this residue in binding these inhibitors and/or NAAG.

TABLE 2

Putative substrate ligands targeted for substitution

Amino acids proposed to make up part of the specificity pocket in GCP II are based on the corresponding residues observed in the crystal structure for the Vibrio aminopeptidase (Chevrier et al., 1994). Assignment of residues in Streptomyces is based on the superimposition and amino acid sequence alignment to the Vibrio aminopeptidase (Greenblatt et al., 1997). The carbonyl oxygen of Arg-202 in Streptomyces hydrogen bonds with the zinc bound $H_2PO_4^-$. In contrast to putative zinc ligands and adjacent residues that are indicated in Table 1, putative substrate ligands are not conserved. See legend for Table 1 for description of Comments.

GCP II	*Streptomyces*	*Vibrio*	Comments
Arg-463	Asp-173	Ile-193	
Lys-499	Glu-198	Cys-223	
Lys-500			
Ser-501	Asp-200	Tyr-225	Hydroxamate
Asn-519	Arg-202	Cys-227	$H_2PO_4^-$
Arg-536	Gly-217	Met-242	
Thr-538	Phe-219	Phe-244	
Lys-545	Gly-223	Phe-248	

TABLE 3

Summary of substitutions to putative zinc ligands and nearby residues

Single substitutions are indicated along with the resultant enzyme activity using [^{3}H]NAAG as substrate; "no" indicates no detectable enzyme activity, even after incubations of 16 h. Lower case "yes" indicates very little but detectable activity such that reliable kinetic parameters could not be obtained. See Table 4 for kinetic parameters for mutants indicated by "Yes". Italics indicate slightly altered migration observed in an immunoblot.

GCP II	Substitution/Activity						Comments
His-377	Gly	no	Ala	no[a]	Gln	no[a]	Zn^{2+}/Hg^{2+}
Asp-379	Glu	*no*[a]	Asn	*no*[a]			H-bond
Asp-387	Glu	no	Asn	Yes	Leu	*no*[a]	Zn^{2+}/Hg^{2+} bridging
Pro-388	Ala	Yes					cis bond
Glu-424	Gln	Yes	Asp	yes[a]			PO_4^{2-}/hydroxamate
Glu-425	Gln	no[a]	Asp	no[a]			Zn^{2+}
Asp-453	Glu	yes[a]	Asn	*no*[a]	Leu	*no*[a]	Zn^{2+}/Hg^{2+}
Ser-454	Ala	Yes					
Tyr-552	Phe	Yes					PO_4^{2-}
His-553	Gly	no	Ala	no	Gln	no[a]	Zn^{2+}

[a] Indicates a low level of expression in an immunoblot, see Fig. 2A for examples. See legend for Table 1 for description of comments.

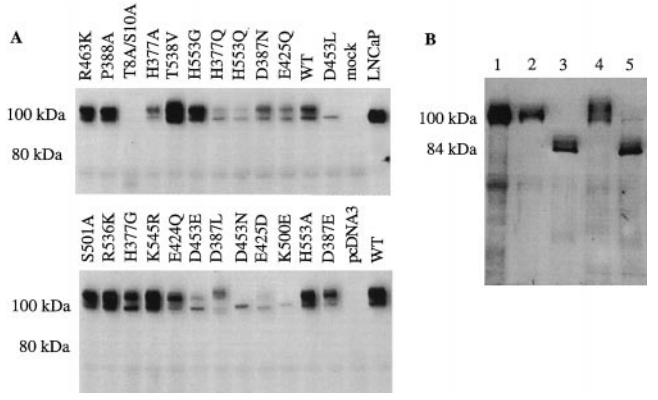

Fig. 2. Immunoblot analysis. A, approximately 10 μg of total protein from whole-cell lysates from representative mutants were loaded and compared to native enzyme (WT). The region shown is from about 70 to 120 kDa. B, deglycosylation of native enzyme in whole-cell lysates compared with the isotype expressed in LNCaP cells. Lane 1, LNCaP no treatment; lane 2, LNCaP incubated without glycosidase; lane 3, LNCaP with glycosidase; lane 4, transfected sample incubated without glycosidase; and lane 5, transfected sample incubated with glycosidase.

Immunoblot Analysis. To determine whether mutant protein was expressed, immunoblot analysis was performed. Mutant protein was expressed even for those mutants that showed no activity (Fig. 2A). Two bands observed in the immunoblot suggest that two different species were present. One explanation for the two bands is differential glycosylation. To test this, the lysate from cells transfected with wild-type cDNA (i.e., expression of native enzyme) was deglycosylated under denaturing conditions and run on a gel for immunoblot analysis. One band was predominately seen at 84 kDa, consistent with the predicted size of the GCP II polypeptide (i.e., deglycosylated protein) (Fig. 2B). The human prostate cancer cell line LNCaP overexpresses GCP II (Israeli et al., 1994). The LNCaP cell lysates expressed one

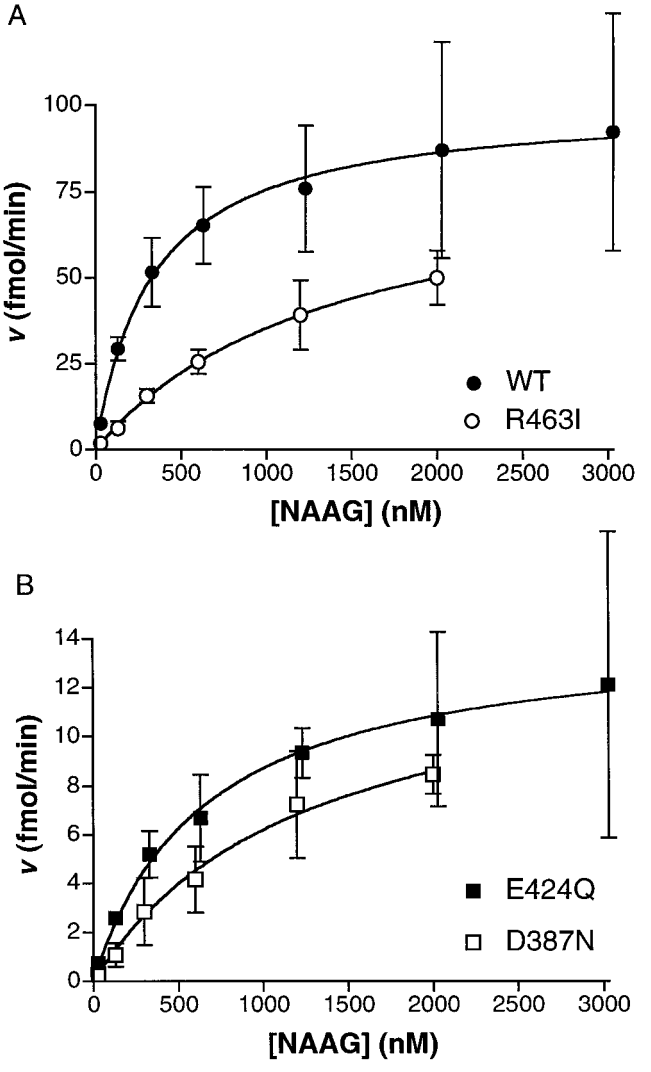

Fig. 3. Michaelis-Menten kinetics. Examples are given of saturation kinetics from whole cell lysates. Two micrograms of total protein was assayed in the presence of a fixed amount of [^{3}H]NAAG. Error bars for the initial velocity represent the S.E.M. of the 95% confidence interval of the slope of the product versus time curve. A, native enzyme (WT) and a representative substitution to a residue proposed to bind substrate, R463I. B, substitutions to the putative catalytic Glu-424, E424Q, and the putative bridging ligand Asp-387, D387N.

7E11-C5 immunoreactive species that migrated at a position that is in between the two bands from the transfected samples. Upon deglycosylation this band migrated at the same position as the deglycosylated transfected sample (Fig. 2B).

The migration pattern of the two bands around 100 kDa in the immunoblot gives an indication of the glycosylated state. A band at 84 kDa would indicate a deglycosylated form. None of the mutants showed a band around 84 kDa, suggesting that all of the mutants are glycosylated (Fig. 2A). To test whether glycosylation may influence enzyme activity, the putative glycosylation site Asn-459, which is near the putative Zn^{++} ligand Asp-453, was substituted to Asp. The two bands observed in an immunoblot ran slightly faster than wild-type protein, indicating an alteration in the glycosylated state (data not shown). The N459D mutant also had slightly altered kinetic parameters (Table 4) and a 2-fold increase in the IC_{50} for pteroylpenta-γ-glutamate (Table 5). In general, anomalous band migration (e.g., D387L in Fig. 2A) in the immunoblot, indicated by italics in Tables 3 and 4, correlated with no detectable activity, with the exception of N459D. For those mutants for which kinetic parameters were obtained, the two bands seen in the immunoblot migrated with wild-type protein, suggesting that glycosylation had not drastically changed and that the affect of the mutation was the result of the substitution and not due to a change in glycosylation.

TABLE 4

Kinetic parameters obtained for mutants

The Michaelis-Menten parameters K_m and V_{max} for NAAG were determined by saturation kinetics for mutants and compared with native enzyme wild type (WT), see Fig. 3 for examples. V_{max} has been adjusted by the relative intensities of protein expression quantitated by an immunoblot by the ratio of WT to mutant. Italics indicate slightly altered migration observed in an immunoblot.

	K_m	V_{max}
	nM	*fmol/min*
WT	330 (267–393)	101 (95–106)
Zn^{2+} ligands and nearby residues		
D387N	1475 (670–2280)	24 (18–31)
P388A	>3000	ND
E424Q	650 (489–812)	14 (13–16)
S454A	90 (61–119)	35 (22–37)
Y552F	527 (196–934)	26 (19–33)
Substrate ligands		
R463K	328 (188–468)	104 (91–117)
R463I†	1580 (1410–1750)	90 (83–94)
K499E	193 (117–269)	118 (108–129)
K500R	471 (267–675)	142 (121–165)
K500E[a]	ND	ND
S501A	332 (224–440)	77 (70–83)
N519D	ND	ND
R536K	266 (214–318)	84 (78–89)
R536E	>3000	ND
T538V	1341 (1113–1569)	99 (90–108)
K545R	272 (250–294)	132 (129–135)
K545E	1166 (917–1415)	73 (65–80)
Glycosylation		
N459D	387 (189–586)	50 (42–58)

[a] Indicates low level of expression in an immunoblot. ND, indicates not determined. The 95% confidence limits are presented in parentheses.

TABLE 5

IC_{50} values for pteroylpenta-γ-glutamate

IC_{50} was determined for the alternative substrate, pteroylpenta-γ-glutamate for selected mutants. IC_{50} value was determined by varying the concentration of inhibitor in the presence of 1 mM Co^{2+} and 10 nM [^{3}H]NAAG where the 95% confidence interval is shown in parentheses.

	IC_{50}
	nM
WT	85 (56–127)
Zn vicinity	
D387N	249 (76–818)
P388A	174 (56–544)
E424Q	124 (76–204)
S454A	97 (68–139)
Substrate	
R463I	128 (95–173)
K500R	148 (110–200)
R536E	705 (368–1348)
T538V	86 (59–125)
K545E	768 (606–973)
N-Glycos	
N459D	170 (94–305)

Discussion

Site-directed mutagenesis has been performed in the human gene for GCP II to test assignments of specific amino acids implicated in metal ligand binding, substrate binding, and other structural and functional aspects of enzyme catalysis. Assignments of these residues are based on the amino acid sequence alignment of GCP II to low molecular weight aminopeptidases whose crystal structures have been determined (Chevrier et al., 1994; Rawlings and Barrett, 1997; Greenblatt et al., 1997). These aminopeptidases from *S. griseus* and *V. proteolyticus* are cocatalytic zinc metallopeptidases that are members of the peptidase family M28. Zinc ligands are conserved between these aminopeptidases and GCP II (Table 1). However, putative substrate ligands are not conserved (Table 2), consistent with a difference in substrate specificity. All residues targeted for mutagenesis that resulted in altered kinetic parameters, including putative substrate ligands, are conserved among the human, rat, and pig.

Substitutions to Putative Zinc Ligands. Single substitutions have been designed at each of the five putative Zn^{++} ligands (Table 3). A topological diagram, based on the *Vibrio* aminopeptidase structure, is shown in Fig. 4 summarizing the mutagenesis results and indicating the corresponding ligands in GCP II. In general, substitutions to putative zinc ligands are more disruptive to enzyme activity and stability as detected by immunoblot analysis than are substitutions to putative substrate ligands. It is not uncommon for apo-proteins to be less stable than their holoenzyme. For example, increased protease susceptibility was observed in the apoenzyme of a mutated zinc binding site of peptide deformylase from *Escherichia coli* (Meinnel et al., 1995).

The only GCP II mutant in which substantial activity was observed is for the putative bridging ligand, D387N. The altered kinetic parameters for the D387N mutant suggest

TABLE 6

IC_{50} values for inhibition of the Y552F mutant

The potent inhibitor PMPA is a glutamate analog with a phosphate substitution at the amine position (Jackson et al., 1996). Phosphate ($H_2PO_4^-$) is a low potency inhibitor. Pteroylpenta-γ-glutamate (PPG) is also hydrolyzed by GCP II (Pinto et al., 1996). Glutamate (Glu) is a product of NAAG hydrolysis. β-NAAG is a nonhydrolyzable NAAG analog. Conditions are described in the legend for Table 5.

	IC_{50}	
	Wild type	Y552F
PMPA (nM)	0.9 (0.6–1.4)	75 (52–109)
$H_2PO_4^-$ (mM)	0.5 (0.4–0.7)	9.0 (4.5–17.9)
PPG (nM)	85 (56–127)	19 (10–37)
Glu (μM)	77 (34–175)	15 (14–17)
β-NAAG (μM)	1.2 (0.6–2.6)	2.3 (1.3–4.1)

that this important residue plays either an indirect or direct role in catalysis. Although there is as yet no direct evidence for the perturbation of metal coordination in mutants containing substitutions to putative metal ligands, the results are consistent with the observation that known zinc ligands are highly conserved in the sequence alignment of the peptidase family M28.

Substitutions to Residues Next to Putative Zinc Ligands. Amino acid residues next to metal ligands can affect the local structure and/or function of the enzyme. In the crystal structures of the *Streptomyces* and *Vibrio* aminopeptidases, the corresponding Asp-379 is shown to hydrogen bond to His-377. There may be a requirement for the proper positioning or electronic interaction of His-377 such that substitution of Asp-379 to Glu or Asn dramatically perturbs the local structure and/or function (Table 3). This triad feature (e.g., Asp-His-Zn^{++}) is also found in other proteases such as the mononuclear zinc site of thermolysin in which both zinc-associated histidines are also coordinated by either an Asn or Asp. It has been proposed that the active site of neutral endopeptidase (NEP) has a similar structure to thermolysin (Benchetrit et al., 1988). A substitution similar to the present case in NEP also decreased enzyme activity in which the corresponding Asp of the triad (i.e., Asp-650) was mutated to Glu, Asn, or Ala, (Le Moual et al., 1994).

A nonproline *cis*-peptide bond that involves the backbone of the bridging aspartic acid ligand is observed in the crystal structure of the *Vibrio* and *Streptomyces* aminopeptidases and carboxypeptidase G_2. As pointed out by Rawlings and Barrett (1997), a proline, which is more likely to accommodate a *cis*-peptide bond, is at this corresponding position in GCP II next to the putative bridging zinc ligand Asp-387. The large increase in K_m (>3 μM) for substitution to Ala suggests that Pro-388 plays an important structural role in the active site of GCP II that most likely affects substrate binding indirectly.

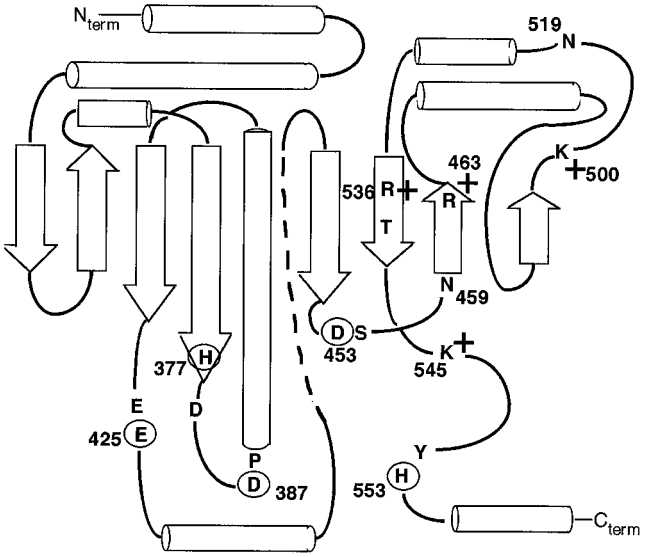

Fig. 4. Predicted topological diagram of the catalytic domain of GCP II. The predicted catalytic domain shown is from residues 287 to 587. Regions of secondary structure are shown when aligned to the *Vibrio* aminopeptidase. Arrows indicate β-sheets and cylinders α-helices. A summary of substitutions that resulted in altered enzyme activity is indicated: 1) The putative zinc ligands are circled with their corresponding positions indicated. 2) Neighboring residues to the putative zinc ligands are indicated in bold. 3) Positively charged residues thought to bind substrate are indicated in bold and a plus sign. 4) Two other residues implicated in substrate binding are Asn-519 and Thr-538. Asn-459 is one of three putative glycosylation sites located in the catalytic domain.

Substitution of Glu-424 to Gln resulted in a decrease in V_{max} suggesting a role for this carboxylate in catalysis. In the *Vibrio* aminopeptidase, the corresponding glutamate (Glu-151) has been proposed to be a general base in the catalytic mechanism and has been shown to be involved in binding to the bridging H_2O or phosphate or to a hydroxamate inhibitor (Table 1) (Chevrier et al., 1996). In the mononuclear carboxypeptidase A and thermolysin, a glutamate residue, implicated in the catalytic mechanism, is in a HEXXH motif in which the Glu is the putative catalytic residue and the two His are Zn^{++} ligands. Substitutions of Glu to Asp or Gln in this motif in peptide deformylase and NEP resulted in decreased activity (Devault et al., 1988; Meinnel et al., 1995).

Both Ser-454 and Tyr-552 may comprise part of the substrate-binding site because their corresponding residues in the *Vibrio* aminopeptidase help define a specificity pocket. In addition, these amino acids are directly next to putative zinc ligands, and the corresponding Tyr-552 in the *Streptomyces* aminopeptidase has been shown in the crystal structure to hydrogen bond with phosphate that is bound between the two zinc ions. The reduced V_{max} suggests that these residues, like Glu-424, are important for enzymatic activity. However, the corresponding Ser-454 and Tyr-552 are not conserved (Table 1). These substitutions may indirectly perturb the local structure or reflect mechanistic differences unique to each particular peptidase. Interestingly, the large increase in the IC_{50} for PMPA or phosphate in the presence of NAAG may indicate that the Tyr-552 hydroxyl is important for the binding of these inhibitors. PMPA is a glutamate analog with a phosphate substitution at the amine position (Jackson et al., 1996). Tyr-552 may possibly bind to the phosphate functionality of PMPA because phosphate inhibition was also perturbed in the Y552F mutant.

Putative Substrate-Binding Determinants. Four positively charged residues in GCP II have been predicted by Rawlings and Barrett (1997) to be involved in the binding of the negatively charged substrates. The corresponding residues in the *Vibrio* aminopeptidase make up part of the hydrophobic substrate specificity pocket. The present data support the assignment of these specificity determinants. Because many residues are involved in substrate binding, it might be expected that any one residue would contribute only partially to the overall affinity for substrate. In this case, a single substitution would not be expected to eliminate binding. The data support this concept, because certain substitutions alter but do not abolish activity. Only when the substitution was a large charge perturbation, such as Lys to Glu, has a large change in K_m been observed. The only prediction not substantiated was for Lys-499. However, this amino acid is not conserved in the rat or pig sequence (Bzdega et al., 1997; Halsted et al., 1998; Luthi-Carter et al., 1998). Interestingly, there is another Lys conserved in the rat and pig sequences directly next to Lys-499 at position 500 wherein substitution to Glu resulted in a loss of enzyme activity. Location of these putative substrate binding residues is shown in Fig. 4. An exchange of Lys and Arg did not seem to perturb substrate binding (Table 4), supporting the role of the positively charged nature of these residues in binding. Altered binding of pteroylpenta-γ-glutamate by some of these mutants indicates that NAAG and folylpolyglutamate may share com-

mon binding determinants. Our data indicate that specific residues, including positively charged ones, influence substrate binding either directly or indirectly and are consistent with the model proposed by Rawlings and Barrett (1997).

Identification of Important Structural and Functional Elements through Evolutionary Conservation. Important structural similarities are often identified by similarities between mammalian and bacterial proteins. Interesting examples for which mutagenesis studies have been conducted include both metabotropic and ionotropic glutamate receptors, such as the *N*-methyl-D-aspartate receptor in which similarities to bacterial amino acid binding proteins have been observed (O'Hara et al., 1993; Kuryatov et al., 1994; Stern-Bach et al., 1994; Paas et al., 1996). As mentioned previously, structural similarities have been identified between NEP, a type II membrane zinc metallopeptidase, and the mononuclear zinc containing thermolysin (Benchetrit et al., 1988). Mutagenesis analyses of NEP support assignments made from the sequence alignment even though little amino acid identity exists between the two sequences (Marie-Claire et al., 1997 and references therein). These studies, like the current one, suggest that the three-dimensional structure of the mammalian proteins are similar to their bacterial counterparts and that structural and functional elements can be predicted based on these comparisons. Lastly, our data from the mutagenesis studies may provide useful information to aid in the design of pharmacologic reagents.

Acknowledgments

We thank Drs. Gerald Murphy and Alton Boynton for the monoclonal antibody 7E11-C5, Drs. Rudy Tanzi and Robert Moir for assistance in quantitating immunoblots, Dr. Craig Martin for discussion on kinetic analysis, and Drs. Neil Rawlings and Alan Barrett for review of the manuscript.

References

Benchetrit T, Bissery V, Mornon JP, Devault A, Crine P and Roques BP (1988) Primary structure homologies between two zinc metallopeptidases, the neutral endopeptidase 24.11 ("enkephalinase") and thermolysin, through clustering analysis. *Biochemistry* **27:**592–596.

Berger UV, Carter RE, McKee M and Coyle JT (1995a) *N*-acetylated alpha-linked acidic dipeptidase is expressed by non-myelinating Schwann cells in the peripheral nervous system. *J Neurocytol* **24:**99–109.

Berger UV, Carter RE and Coyle JT (1995b) The immunocytochemical localization of *N*-acetylaspartylglutamate, its hydrolyzing enzyme NAALADase, and the NMDAR1 receptor at a vertebrate neuromuscular junction. *Neuroscience* **64:**847–850.

Burlina AP, Skaper SD, Mazza MR, Ferrari V, Leon AL and Burlina AB (1994) *N*-acetylaspartylglutamate selectively inhibits neuronal responses to *N*-methyl-D-aspartic acid in vitro. *J Neurochem* **63:**1174–1177.

Bzdega T, Turi T, Wroblewska B, She D, Chung HS, Kim H and Neale JH (1997) Molecular cloning of a peptidase against *N*-acetylaspartylglutamate from a rat hippocampal cDNA library. *J Neurochem* **69:**2270–2277.

Carter RE, Feldman AR and Coyle JT (1996) Prostrate-specific membrane antigen is a hydrolase with substrate and pharmacologic characteristics of a neuropeptidase. *Proc Natl Acad Sci USA* **93:**749–753.

Chevrier B, D'Orchymont H, Schalk C, Tarnus C and Moras D (1996) The structure of the *Aeromonas proteolytica* aminopeptidase complexed with a hydroxamate inhibitor: Involvement in catalysis of Glu-151 and two zinc ions of the co-catalytic unit. *Eur J Biochem* **237:**393–398.

Chevrier B, Schalk C, D'Orchymont H, Rondeau J-M, Moras D and Tarnus C (1994) Crystal structure of *Aeromonas proteolytica* aminopeptidase: A prototypical member of the co-catalytic zinc enzyme family. *Structure* **2:**283–291.

Devault A, Nault C, Zollinger M, Fournié-Zaluski M-C, Roques BP, Crine P and Boileau G (1988) Expression of neutral endopeptidase (enkephalinase) in heterologous COS-1 cells: Characterization of the recombinant enzyme and evidence for a glutamic acid residue at the active site. *J Biol Chem* **263:**4033–4040.

Graham FL and van der Eb AJ (1973) A new technique for the assay of infectivity of human adenovirus 5 DNA. *Virology* **52:**456–467.

Greenblatt HM, Almog O, Maras B, Spungin-Bialik A, Barra D, Blumberg S and Shoham G (1997) *Streptomyces griseus* aminopeptidase: X-ray crystallographic structure at 1.75 Å resolution. *J Mol Biol* **265:**620–636.

Grunze HCR, Rainnie DG, Hasselmo ME, Barkai E, Hearn EF, McCarley RW and Greene RW (1996) NMDA-dependent modulation of CA1 local circuit inhibition. *J Neurosci* **16:**2034–2043.

Halsted CH, Ling E-H, Luthi-Carter R, Villanueva JA, Gardner JM and Coyle JT (1998) Folylpoly-γ-glutamate carboxypeptidase from pig jejunum: Molecular characterization and relation to glutamate carboxypeptidase II. *J Biol Chem* **273:**20417–20424.

Harukuni I, Bhardwaj A, Hurn PD, Slusher BS and Traystman RJ (1997) Novel NAALADase inhibitor, PMPA, improves infarct volume in experimental stroke. *Soc Neurosci Abst* **23:**898.3.

Israeli RS, Powell CT, Corr JG, Fair WR and Heston WDW (1994) Expression of the prostate-specific membrane antigen. *Cancer Res* **54:**1807–1811.

Israeli RS, Powell CT, Fair WR and Heston WDW (1993) Molecular cloning of a complementary DNA encoding a prostate-specific membrane antigen. *Cancer Res* **53:**227–230.

Jackson PF, Cole DC, Slusher BS, Stetz SL, Ross LE, Donzanti BA and Trainor DA (1996) Design, synthesis, and biological activity of a potent inhibitor of the neuropeptidase *N*-acetylated α-linked acidic dipeptidase. *J Med Chem* **39:**619–622.

Kunkel TA, Bebenek K and McClary J (1991) Efficient site-directed mutagenesis using uracil-containing DNA. *Methods Enzymol* **204:**125–139.

Kuryatov A, Laube B, Betz H and Kuhse J (1994) Mutational analysis of the glycine-binding site of the NMDA receptor: Structural similarity with bacterial amino acid-binding proteins. *Neuron* **12:**1291–1300.

Le Moual H, Dion N, Roques BP, Crine P, and Boileau G (1994) Asp650 is crucial for catalytic activity of neutral endopeptidase 24–11. *Eur J Biochem* **221:**475–480.

Luthi-Carter R, Berger UV, Barczak AK, Enna M and Coyle JT (1998) Isolation and expression of a rat brain cDNA encoding glutamate carboxypeptidase II. *Proc Natl Acad Sci USA* **95:**3215–3220.

Marie-Claire C, Ruffet E, Antonczak S, Beaumont A, O'Donohue M, Roques BP and Fournié-Zaluski M-C (1997) Evidence by site-directed mutagenesis that arginine 203 of thermolysin and arginine 717 of neprilysin (neutral endopeptidase) play equivalent critical roles in substrate hydrolysis and inhibitor binding. *Biochemistry* **36:**13938–13945.

Meinnel T, Lazennec C and Blanquet S (1995) Mapping of the active site zinc ligands of peptide deformylase. *J Mol Biol* **254:**175–183.

O'Hara PJ, Sheppard PO, Thøgersin H, Venezia D, Haldeman BA, McGrane V, Houamed KM, Thomsen C, Gilbert TL and Mulvihill ER (1993) The ligand-binding domain in metabotropic glutamate receptors is related to bacterial periplasmic binding proteins. *Neuron* **11:**41–52.

Paas Y, Eisenstein M, Medevielle F, Teichberg VI and Devillers-Thiéry A (1996) Identification of the amino acid subsets accounting for the ligand binding specificity of a glutamate receptor. *Neuron* **17:**979–990.

Pinto JT, Suffoletto BP, Berzin TM, Qiao CH, Lin S, Tong WP, May F, Mukherjee B and Heston WDW (1996) Prostate specific membrane (PSM) antigen: A novel member of folate hydrolase in human prostatic carcinoma cells. *Clin Cancer Res* **2:**1445–1451.

Puttfarcken PS, Montgomery D, Coyle JT and Werling LL (1993) *N*-acetyl-L-spartyl-L-glutamate (NAAG) modulation of NMDA-stimulated [^{3}H]norepinephrine release from rat hippocampal slices. *J Pharmacol Exp Ther* **266:**796–803.

Rawlings ND and Barrett AJ (1997) Structure of membrane glutamate carboxypeptidase. *Biochim Biophys Acta* **1339:**247–252.

Robinson MB, Blakely RD, Couto R and Coyle JT (1987) Hydrolysis of the brain dipeptide *N*-acetyl-L-aspartyl-L-glutamate: Identification and characterization of a novel *N*-acetylated α-linked acidic dipeptidase activity from rat brain. *J Biol Chem* **262:**14498–14506.

Rowsell S, Pauptit RA, Tucker AD, Melton RG, Blow DM and Brick P (1997) Crystal structure of carboxypeptidase G_2, a bacterial enzyme with applications in cancer therapy. *Structure* **5:**337–347.

Sekiguchi M, Okamoto K and Sakai Y (1989) Low-concentration *N*-acetylaspartylglutamate suppresses the climbing fiber response of Purkinje cells in Guinea pig cerebellar slices and the responses to excitatory amino acids of Xenopus laevis oocytes injected with cerebellar mRNA. *Brain Res* **482:**87–96.

Serval V, Barbeito L, Pittaluga A, Cheramy A, Lavielle S and Glowinski J (1990) Competitive inhibition of *N*-acetylated-alpha-linked acidic dipeptidase activity by *N*-acetyl-L-aspartyl-β-linked-L-glutamate. *J Neurochem* **55:**39–46.

Slusher BS, Robinson MB, Tsai G, Simmons M, Richards SS and Coyle JT (1990) Rat brain *N*-acetylated alpha-linked acidic dipeptidase activity: Purification and immunologic characterization. *J Biol Chem* **265:**21297–21301.

Slusher BS, Tsai G, Yoo G and Coyle JT (1992) Immunocytochemical localization of the *N*-acetyl-aspartyl-glutamate (NAAG) hydrolyzing enzyme *N*-acetylated α-linked acidic dipeptidase (NAALADase). *J Comp Neurol* **315:**217–229.

Stauch BL, Robinson MB, Forloni G, Tsai G and Coyle JT (1989) The effects of *N*-acetylated alpha-linked acidic dipeptidase (NAALADase) inhibitors on [^{3}H]NAAG catabolism in vivo. *Neurocsci Lett* **100:**295–300.

Stern-Bach Y, Bettler B, Hartley M, Sheppard PO, O'Hara PJ and Heinemann SF (1994) Agonist selectivity of glutamate receptors is specified by two domains structurally related to bacterial amino acid-binding proteins. *Neuron* **13:**1345–1357.

Troyer JK, Beckett ML and Wright GL Jr (1995a) Detection and characterization of the prostate-specific membrane antigen (PSMA) in tissue extracts and body fluids. *Int J Cancer* **62:**552–558.

Troyer JK, Feng Q, Beckett ML and Wright GL Jr (1995b) Biochemical characterization of the 7E11–C5.3 epitope of the prostate-specific membrane antigen. *Urol Oncol* **1:**29–37.

Vallee BL and Auld DS (1993) Cocatalytic zinc motifs in enzyme catalysis. *Proc Natl Acad Sci USA* **90:**2715–2718.

Wroblewska B, Wroblewski JT, Pshenichkin S, Surin A, Sullivan SE and Neale JH (1997) *N*-acetylaspartylglutamate selectively activates mGluR3 receptors in transfected cells. *J Neurochem* **69:**174–181.

Send reprint requests to: Dr. Joseph Coyle, McLean Hospital, 115 Mill St., Belmont, MA 02178. E-mail: jcoyle@warren.med.harvard.edu